Asian Journal of Information Technology 15 (16): 3125-3133, 2016
ISSN: 1682-3915


# Tbann: Tree Bagger Algorithm with Neural Network-Based Hyperspectral Images Classification

[1]Devabalan and [2]R. Saravanan
[1]Department of Information Technology,
NPR College of Engineering and Technology, Natham, Dindigul, Tamil Nadu, India
[2]Department of Computer Science and Engineering,
RVS Educational's Trusts Group of Institutions, Dindigul, Tamil Nadu, India

**Abstract:** Geological information prediction and Earth monitoring by the satellite images are the recent research area to preserve the vegetation, weather forecast, and the disaster management. The employment of Hyper Spectral Image (HSI) by capturing the electromechanical energy variations from the Earth's surface in the various spectral bands offers the significant contribution to the remote sensing applications. The clear image analysis depends on the spectral response. The capture of response in HSI in narrow bandwidth causes the less performance. Hence, the number of bands over the various time periods are the important requirement in clear image analysis. The multi-temporal images contain more information than RGB image since more bands are available in it. The absence of frames update leads to accuracy degradation. This study focuses on multi-temporal images for better isolation of normal and noise region and provides the clear image analysis compared to HSI. This study proposes the cellular automata-based noise filtering technique with the changes in noise prediction structure to eradicate the noise components, thereby better isolation is achieved. This study overcomes the update and accuracy limitations by an employment of image fusion to each band to eliminate the cloud and provide the necessary updated frames. The classification of normalized images from the fused images by using Tree Bagger algorithm with Neural Network (NN) formation (TBANN) predicts the cluster label for the color features of specific band results in the reduction of the atmospheric and signal dependent noise. The comparative analysis between the proposed TBANN with the existing methods regarding the accuracy, Kappa coefficient and the number of pixels count assures the effectiveness of TBANN in remote sensing applications.

**Key words:** Hyper Spectral Image (HSI), preprocessing, image fusion, cloud elimination, tree bagger Algorithm, Neural Network (NN)

## INTRODUCTION

Remote imaging spectrometry plays the significant role in geological and ecological research studies that include the spectral features and the object classification. The fundamental process for the remote sensing applications is the extraction of electromagnetic energy from the Earth's surface, spatial, spectral and temporal variations in the field. The understandable feature space creation is the key component for theclassification process. An optical imaging technique operated under infrared and visible range is referred as Hyperspectral Imaging (HSI). The absolute and precise information analysis depends on the clear and detailed spectral response with the narrow bandwidth. Prior to HSI analysis, the radiometric calibration is the fundamental task. The classification techniques applied on HSI involves the discriminative spectral bands and a large number of features. The integration of spatial and spectral features is the challenging task in HSI analysis.

The high dimensionality of HSI data may increase the size of computational operations. Therefore, it influences the classification performance. The data widely used to monitor the Earth activities is referred as Landsat data. For the same locations, a large number of available HSI in different time periods offer the clear analysis. The presence of cloud, cloud shadow and snow in Landsat images makes the optical sensor utilization in abetter way. The brightness effect of cloud/snow and the darkness of the cloud shadow have the great impact on spectral bands handling. The execution of remote sensing activities depends on the performance of change detection, cloud/cloud shadow removal. The accurate

**Corresponding Author:** Devabalan, Department of Information Technology, NPR College of Engineering and Technology, Natham, Dindigul, Tamil Nadu, India

decision is the necessary. The information collection from the pixel variations offers the better performance for wide variations. The dependency existence between the pixel contents identification and the spectral information depends on the proper geometric relationship. The reduction in a number of pixels for the linear number of spectral bands reduces the data volume.

Spectral information identification and the optimal wavelength identification are the important techniques to reduce the dimensionality in HSI. In HSI, the hyperspectral sensors capture the Electromagnetic energy from the earth's surface, spectral and spatial variations. The spatial resolution variations depend on the high altitude and wide area coverage degrades the image quality adversely. The relevancy prediction of small objects is the necessary task of an accurate classification due to the spatial resolution existence. The rich information identification in HSI depends on the estimation of thedistinguishingrelationship between the spectral similar materials. The prior assumption of class labels for each spectral signature in supervised classification approach is not suitable due to the unfavorable ratio between the large spectral bands and the small training samples.

The exploration of ground truth information is not common for diverse training samples due to the expensive collection of reliable samples. Kernel methods and the machine learning techniques require an enhancement to reduce the data dimensionality. The bounding of convex combinations in the composite kernels and the optimization of parameters are the difficult tasks. The presence of nonlinearities due to the atmospheric and geological conditions and the fewer training samples availabilities causes the classification task as the challenging problem.

The description of surface features via hyperspectral image is the less efficient due to the narrow bands that lead to broad wavelength image category called Multi-spectral imagery. This study focusses on the multi-spectral image classification with the suitable cloud removal and classification techniques. The multi-spectral aspect of image classification achieves the clear analysis because of the simultaneous timely (year, day, month) and spectral bands capturing. The technical contributions of proposed work are listed as follows:

- The employment of cellular automata based noise filtering technique with changes in noise prediction structure reduces the atmospheric and signal-dependent noises
- An image fusion technique based on the frame difference level eradicates the cloud and cloud shadow efficiently
- The integration of Tree-Bagger algorithm with Neural Network (TBANN) in this study forms the cluster of normalized images by using cluster label prediction of the color features
- Finally,the comparative analysis between proposed method and existing algorithms assure the effective cloud removal and better classification performance

**Literature review:** This section reviews the relevant literature on the classification of Hyper Spectral Images (HSI) based on various techniques.The classification in remote sensing applications includes the rich and meaningful feature space creation that leads to the spectral-spatial classification scheme. Knauer and colleagues discussed the various classification techniques for low dimensional datasets. They proposed the real-world test case for the proposed approach. The bias variations and the decomposition are the difficult processes in HSI classification. Merentitis *et al.* (2014) introduced the unified framework for the provision of theoptimal trade-off between the bias variations and the decomposition. They jointly optimized the classification steps to achieve the trade-off. The large spectral variability and the spatial variations existence in HSI introduced the tiny regions and the labeling of these regions is the difficult task. Bai *et al.* (2013) applied the pixel-wise classification approach with the Support Vector Machine (SVM) which results in the preservation of pixels with high probabilities. They tested the small training sets with the graph cut approach to assure the robustness. The impact of magnetite minerals, cloud and cloud shadow were high and they limited the useful information prediction. The multiple queries scanning is the difficult task over the large size images. Patterson *et al.* (2016) described the efficient framework to support multiple scanning queries for the large size data. They described the preliminary analysis for anomalies detection that required the radial calibration. Ganesh *et al.* (2013) included the calibration with the atmospheric radiation, thereflectance for satellite data preprocessing.

The automatic species mapping depends on the atmospheric variations affected the classification performance adversely. Nia *et al.* (2015) applied the three preprocessing techniques such as atmospheric correction, Gaussian filter, and shade vegetation filters to improve the classification accuracy. Moreover, the accuracy depends on the spectral responses from the utilized sensors in HSI. The narrow bands spectral response degrade the classification accuracy and the less performance in image analysis that initiate the multi-temporal images handling. The trade-off between the high-accuracy and the cloud masking was the significant task in themulti-temporal image. Zhu and Woodcock (2014) discussed the

Automated Tmask algorithm for cloud/cloud shadow removal. The comparison of cloud models with the landstate observations offered the better cloud removal performance. The utilization of Land site satellite images in the Land Use/Land Cover (LULC) contained several degree of cloud covers that contained locational and the class labeling errors. Johnson and Iizuka (2016) discussed the noise tolerant algorithms such as Naive Bayesian (NB), decision tree (C4.5) algorithm and the random forest to eradicate the high noise levels and the degree of cloud cover. Research studies extended the application of HSI to the object determination of pork quality grades. Barbin *et al.* (2012) carried out the Principal Component Analysis (PCA) within the particular wavelength ranges to produce the classification maps. The increase in spectral resolution of HSI opened the new research studies in HSI analysis. Valls *et al.* (2014) investigated the HSI classification problems due to the noise effects.

The multi-variant scenarios and the spatial dependence of the pixels increased the dimensionality of training datasets. Forero *et al.* (2013) presented the pixel-wise classification with the joint usage of spectral and spatial information. They proposed the Additive Morphological Decomposition (AMD) based on the morphological operators. Low spatial resolution caused the problems in structured detection and the unsupervised classification. Villa *et al.* (2013) exploited the rich information prediction problem due to the imperfect image optics and illumination effects. They performed spectral unmixing and the unsupervised classification for thematic maps construction. The accurate thematic maps creation by the automated procedures is the difficult task. Moreno *et al.* (2014) performed the classification in three stages as follows: thetransformation of spectral data into the hyperspherical representation, gradient computation, and the feature selection. They obtained better classification results. The generalization of composite kernels depends on the combination of spectral and spatial information. Li *et al.* (2013) discussed the multi-nominal logistics regression and extended the multi-attribute profiles for spatial/spectral information modeling. The analytical form of multi-class classification introduced the problems. Bazi *et al.* (2014) proposed the efficient machine learning algorithm which is the combination of Differential Evolution and Extreme Learning Machine (ELM) to address the feature selection issues.

The sparse representation based classification for the large dimensional datasets is the inefficient process. Wang *et al.* (2014) investigated the sparse representation model under the probabilistic framework. The spatial class dependence is captured and further refined by using the probabilistic model.The increase in spectral combinations introduced the difficulties in the rich information preserving probabilistic models. Tochon *et al.* (2015) discussed the Binary Partition Tree (BPT) algorithm in different strategies to reduce the dimensionality of large datasets. They employed the principal component analysis and comparison of the various components to reduce the data dimensionality. The manual tuning of the kernels affected the classification performance severely. Ghamisi *et al.* (2014) discussed the Fractional-Order Darwinian Particle Swarm Optimization (FODPSO) and the mean shift segmentation. The integration of PSO with the mean shift methods reduced the complexities in thekernel that improved the classification accuracy. The lack of labeling and the high-dimensionality are the major problems in the HSI classification. Ji *et al.* (2014) discussed the spectral/spatial constraints to formulate the pixels relationship in hypergraph structure. The utilization of distance among the pixels for the feature-based hyperedge generation to achieve the joint optimization functionality. They also provided the comparative analysis of various kernel-based methods such as Semi-Supervised Graph-based method for Cross Stacked kernel (SSG-CS), SPARSE, Conditional Random Field (CRF), Local Manifold Learning (LML) combined with the k-Nearest Neighbor (LML+kNN) and the Hyperedge analysis based on features (HG Fea) spatial (HGSpa), weighted (HG W) and spatial constraint (HG) methods. HSI classification with a limited number of labeling is the difficult task in kernel approaches. Gao *et al.* (2014) discussed the bilayer graph-based learning framework to address the problems in labeling process. The neighboring pixel relationship identification with the high data dimensionality was achieved and conducted the unsupervised learning. The Bi-Layer Graph-based Learning (BLGL) provided the maximum classification performance compared to the SSG+CS, CRF and LML+kNN. From the study, the cluster formation and separation are challenging one with the pixel variations on each color band. Also, thepresence of noise and cloud degraded the detection of the earth outward for various applications. An effective classification mechanism is required to remove the noise and cloud to provide the better accuracy.

## MATERIALS AND METHODS

**Hyperspectral image classification using a hierarchical tree bagger algorithm with NN:** This section describes the detailed explanation of the proposed new way of classification of hyperspectral images as in Fig.1. The major components of this system are:

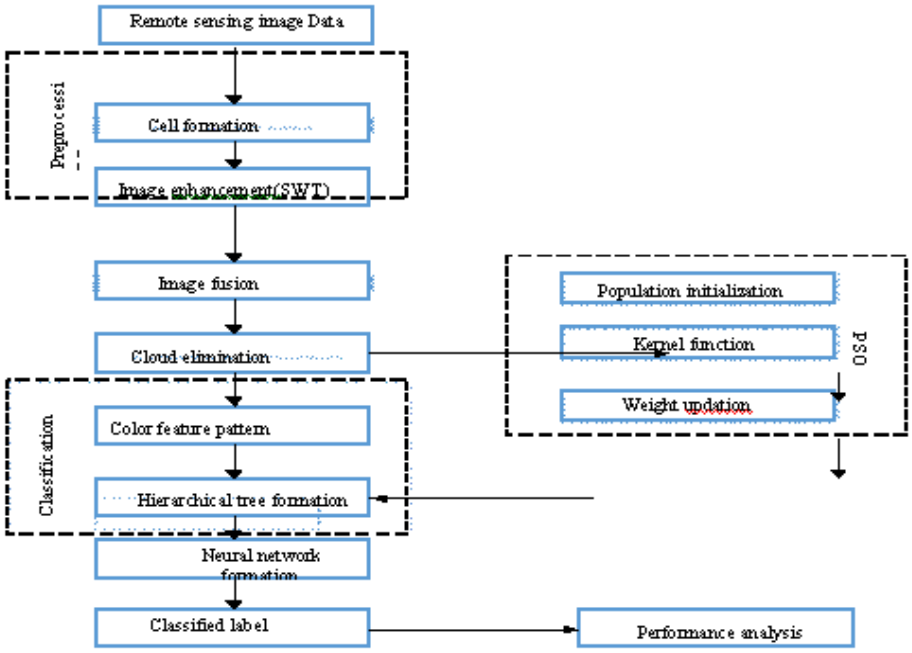


Fig. 1: An overall flow diagram of HSI classification using a hierarchical Tree Baggar Algorithm with the Neural Network (TBANN)

- Preprocessing
- Image fusion
- Cloud elimination
- Classification

**Preprocessing:** A preprocessing or filtering step is applied to minimize the noise. Several research studies are available for structuring efficient noise suppression filters. The preprocessing stage plays a vital role in ultrasound image quality enhancement

**Cellular automata filter:** A group of cells, which assumes p possible states (i.e., pixel colors) that updated instantaneously and iteratively refers cellular automaton (CA). A cell state is disturbed by neighboring cell States, and its global evolution is determined using these local iterations. Once a pixel is detected as noisy one state, the modification to the state of random neighbor. In CA theory, two mutual neighborhoods are employed:

- Moore: 8 pixels square neighborhood
- Von-Neumann: 4-pixel neighborhood

Both neighborhoods defined with many edges and the boundary conditions will explain how the CA iterates. It may either iterate periodic or reflected. In this approach, the reflected boundary condition such that the cell is present at the rightmost edge of the grid. The assumption

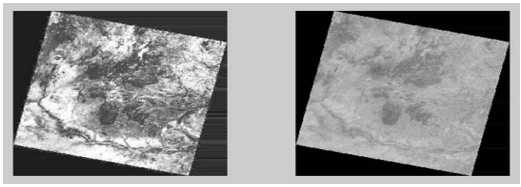

Fig. 2: The input HSI and the preprocessed image

of CA implementation is the presence of neighbor on its right to the cells, which is alike as on the left and similarity for the other edges.

**Histogram equalization:** The equalization techniques applicable to improve the quality of the ultrasound lung image. It eliminates the background information, redundant and hidden details for fast implementation. Also, dealt with contrast enhancement in suspicious areas in the HSI. The result of the preprocessed image is given in the Fig. 2 as follows:

**Image fusion Stationary Wavelet Transform (SWT):** The Stationary Wavelet Transform (SWT) in image fusion process followed by the quality enhancement. Initially, SWT decomposes the given image to single resolution level to detect the cloud. As a result, the flat image and three detailed images such as horizontal, vertical and diagonal images are obtained by in the proposed scheme.

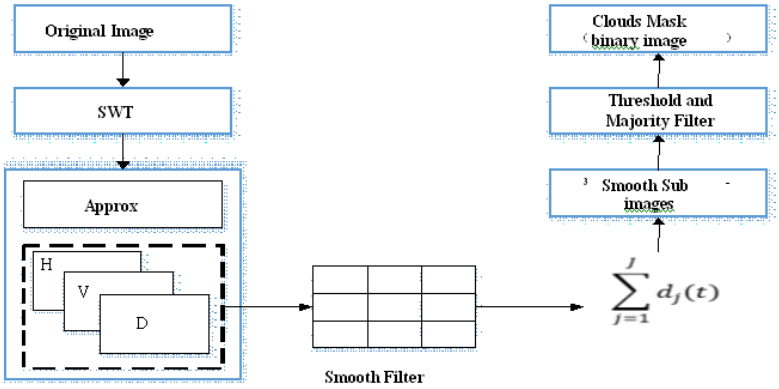


Fig. 3: The process of cloud detection using SWT

The smoothed images obtained from 3×3 low pass filter have the similar resolution as the original image. An application of athreshold to the smoothed images to differentiate the clouds andobtain a new binary. Figure 3 illustrates the SWT-based cloud detection.

**PSO based cloud elimination:** The Particle Swarm Optimization (PSO) performs the cloud elimination followed by an image fusion process. Initially, the initial velocity and the position of the particle is initialized as V = 0.1 and P = $I_e$×V where $I_e$ denotes the preprocessed image. The length of the preprocessed image is assigned to the vector. The coordinate of the particle is predicted by using the following equation:

$$F_{position} = \sum_{i=1}^{n} i = \cos\left((i+1)p + v_i\right)\sum_{j=1}^{m} j\,\mathrm{Cos}\left((j+1)\right) \quad (1)$$

The minimum and maximum value of the positional value are updated with the combination of position and vector. The maximum value of the fitness is formulated as the membership function and then compute the fitness for each particle and iteration. The particle position and vector coordinates are computed for each fitness value. Finally, the affine transform is applied to create the concatenated matrix output.

**Alogorithm 1:** PSO based Cloud Elimination.
Input: Preprocessed Image, '$I_g$
Output: Fused image 'I'
Step 1: Initial velocity, V = 0.1, Initialize particle 'P', P = $I_g$*V.
Step 2: Position of Edges = 'x' and 'y' coordinate points of Edge pixel.
Step 3: Vector = random (length ($I_g$))
Step 4: Coordinate Prediction,

$$F_{position} = \sum_{i=1}^{n} i = \cos\left((i+1)\,p + v_i\right)$$

$$\sum_{j=1}^{m} j\,\mathrm{Cos}\left((j+1)\right)$$

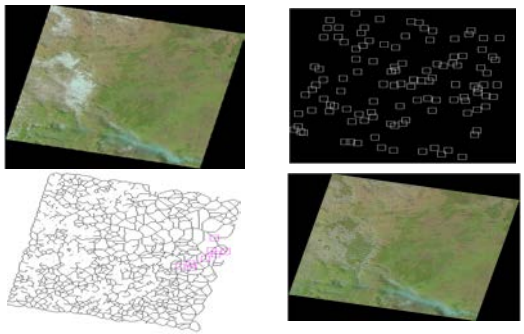

Fig. 4: a) The image before cloud removal; b) Extracted points; c) Collected points; d) The image after cloud removal

// Check fitness forgiven Position by using theobjective function.
Step 5: $L_{position}$ = Minimum (F_Position)
//Check minimum position as $L_{position}$
Step 6: $G_{position}$ = Maximum (F_Position)
//Check maximum position as $G_{position}$
$L_{position}$ = Last Position
$G_{position}$ = Global Position
Step 7: Position = Position + Vector
Step 8: find maximum (fitness_value), mf = max (fitness)//Select index, 'mf'
Step 9: for k = 1 to iteration
Step 10:If Present_fitness<Last_fitness
Step 11: Update $C_{position}$= $L_{position}$
Step 12: End if
Step 13: FP = {P(x,y)}
Step 13: Update Vector and position
Step 14: End loop 'k'.
Step 15: Apply Affine Transform

$$Q = FP_x((FP)_{x-1}...FP_2(FP_1.P))...)$$

Step 16: Matrix Concatenation

$$I_{ij} = a_{il}\ Q_i + b_{il}\ Q_i$$

Figure 4a-d shows the variations of images with the cloud and cloud removal. The periodical positional and velocity update and the new way of membership function

formulation and the affine transformation application efficiently removes the cloud to proceed the clear image analysis.

**Feature extraction:** The extraction of suitable features from the fused image is the next important step in the proposed TBANN framework. This process is split up into two operational stages such as color feature extraction and PSO based feature extraction. The algorithm to compute the color features extraction is listed as follows:

**Alogorithm 2:** Color feature extraction.
Input: Fused image "$I_g$"
Output: Feature set F
Step1: $I_1 = I(M, N, I_1)$
Step2: $I_2 = I(M, N, I_2)$
Step 3: $I_3 = I(M, N, I_3)$
//M, N = Row and Column size of image
//I1, I2, I3 = Sample size of image
Step 4:Calculate the mean, covariance and standard deviation based on the feature vectors
Mean

$$C_{RGB} = I_{RGB}\left(\frac{N \times M}{2}\right)$$ // Covariance

// Standard deviation $$S_{RGB} = \sqrt{\frac{1}{M * N}\sum_{i=1}^{M-N}\left(I_{RGB}(i) - M_{RGB}\right)^2}$$

Step 5:F = $\{M_{rgb}, C_{rgb}, S_{rgb}\}$

Initially, the image coefficients (I1, I2, and I3) are initialized with the row/column and sample image sizes. Then, mean ($M_{RGB}$), Covariance ($C_{RGB}$) and the Standard deviation ($S_{RGB}$) based on the feature vectors computed by using the respective formulas and arranged as the feature set. The best feature selection from the matrix is performed by using the PSO formulation in next section. The algorithm to select the best feature is listed as follows:

**Alogorithm 3:** Color feature extraction.
Input: Feature Matrix, 'Tr'
Output: Best Selection of feature index, 'Fs'
Step1:Initialize Particles, p(x) = $\{p_1(x), P_2(x), ..., P_n(X)\}$
Step 2: Pareto optimal set
$P_{min} = \{p_1(x), P_2(x), ..., P_n(X)\}$
Where,
$p_1(x), P_2(x), ..., P_n(X)$ are 'n' number of objective functions
Step 3: Velocity and position update
$V(i) = C_0 \times V(i-1) + C_1 \times rand\,(p_{best} - p(x)) + C_2 \times r$
$P(x) = P(x) + V(i)$
Step 3: Objective function formulation

$$\eta^{i(k+1,u,q)} = \eta^{i(k,u,q)} + V(i)\phi(K)$$

Where:
L = Present Fitness value of 'η'
M = Average fitness value of 'η'
I = Iteration length.
$\phi(k)$ = Distance value at each position.
$\delta$ = Gradient constant.
Step4: Find anoptimized solution.
If (L<M), then
Update, L=M;
$Q_s = Cost(P_c)$
$\alpha_s = Max(P_c, R)$
Where:
$\alpha_s$ = is the rate of section
$Q_s$ = Interruption cost
R = Permanent interruption
Step 5: $F_s = G(I(P_c(\phi)))$//Extracting index of selected features with probability result from fitness value

The particles represent the features are initialized as (X) = $\{p_1(x), p_2(x), ..., p_n(X)$. The pareto optimal set is created with the position and velocity update. The fitness function formation and the repetitive velocity and positional update extracted the corresponding index of the feature set. The PSO formulation reduces the cost of features extraction.

**Hierarchical tree bagger algorithm with neural network:** The following algorithm shows the hierarchical tree bagger algorithm with the neural network. The tree bagger algorithm contains following processes:

- Data collection
- Feature extraction
- Parameter selection
- Resampling
- Decision tree training
- Classification

The data collection, fusion, and the feature extraction are discussed in the previous study.

**Hierarchical Tree Bagger Algorithm 4**
**Parameter selection criteria:** Choose the parameters for random forest algorithm including the T number of trees and the value for features set variable V(Fs).

**Resampling:** Sample the training data to formulate the tree T with the subsets.

**Decision tree training:**
- A node selects the subset of V(Fs) for a given tree T that represents set of all the predictor measures.
- It provides the optimal split in accordance with the objective function
- At the next node, choose the diverse set of ?at random from all the other predictor measures and repeat the steps

**Label formation:**

$$g_i = \sum_{p=1}^{p}\sum_{m=1}^{M}\left(\frac{\partial Tr(FS)_{p,m}}{\partial t_i} V(FS)_{p,m}\right)$$

Where:
V(FS) = Feature vector of input image with selected attributes

Tr(FS) = Represents Training Feature matrix of Dataset with selected attributes

$g_i$ = Labels corresponds to the segmented output

The benefits of NN-based approaches recognize the HSI classification. NNs are the dominant classification method with nonlinear characteristics and the circumstancethat makes no assumptions about the data distribution. This feature is applicable in cases where no modest phenomenological model exists to defineaccurately the essential physical process that estimates the data distribution. Still, the use of NN for HSI classification has been primarily limited due to the extremely long time requisite to train NN. The training of network includes a small ROI pixel portionwithout requiring a self-determination of ground truth for validation of NN classification results. The testing of classification performance governed by the remaining pixels in ROI.

## RESULTS AND DISCUSSION

This analyzes the proposed methodologyand compares with the existing methods such as SVM, SVM+FODPSO (Gao *et al*., 2014). The input image used for HSI classification in theimageas mentioned in Fig. 5.

The provision of color notification output classifies the satellite image. The classes involved in the proposed TBANNare the mountain, empty land, water, vegetation, and forest. Table 1 depicts the color notifications for various classes such as dark blue denotes the mountain, light blue is an empty land, green is the water, pink is vegetarian, and the yellow denotes the forest.

Figure 6 shows the classification outputs for the existing k-means based classification and proposed TBANN for image 1. Table 2 describes the accuracy analysis for various class labels of Pavia HSI with the existing and proposed TBANN. The comparison shows that the CMA filtering and the PSO-based feature extraction improves the classification performance by 1.9% compared to SVM+FODPSO.

Table 3 presents the number of pixel count and accuracy variations for the existing K-means with PSO[18] and proposed TBANN. The hybrid K-means with PSO efficiently reduces the actual number of pixels for each class of Salians image. The comparative analysis of proposed TBANN with the existing provides the significant improvement in the pixel reduction and accuracy.

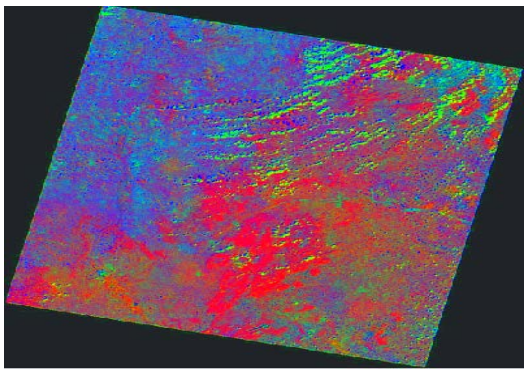

Fig. 5: Hyperspectral image

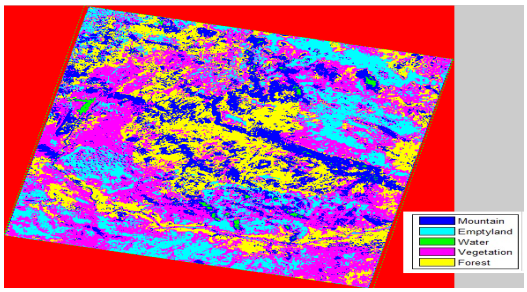


Fig. 6: TBANN output

Table 1: Color notification for five different clusters

| Clusters | Classes | Color notification |
|---|---|---|
| 1 | Water | Blue |
| 2 | Soil | Light shade |
| 3 | Vegetation | Dark Green |
| 4 | Forest | Yellow |
| 5 | Empty Land | Red |

Table 2: Accuracy analysis for various classes of Pavia HSI

| Class | SVM | SVM+FODPSO | TBANN |
|---|---|---|---|
| Asphalt | 94.4 | 96.1 | 98.2 |
| Meadows | 98.1 | 96.9 | 98.7 |
| Gravel | 77.9 | 98.2 | 98.5 |
| Trees | 93.0 | 98.6 | 99.2 |
| Metal Sheets | 99.2 | 99.9 | 100.0 |
| Bare soil | 89.4 | 93.7 | 98.0 |
| Bitumen | 85.8 | 97.9 | 99.4 |
| Bricks | 92.0 | 87.4 | 92.8 |
| Shadow | 99.4 | 99.9 | 100.0 |
| Accuracy | 94.3 | 96.2 | 98.1 |

Figure 7 shows the comparative analysis of proposed TBANN with the existing methods such as HG (Spa, W, Fea), CRF, SSG+CS, LML+KNN and sparse regarding the overall accuracy. The existing HG-W provides more accuracy (93.2 %) for the number of labeled samples compared to the other methods. But, the clear image analysis by using TBANN improves the classification accuracy (93.8 %) further.

Figure 8 shows the Kappa coefficient analysis against the labeled samples for the proposed TBANN and

Table 3: Pixel count and accuracy analysis

| Classes | Number of Pixel Count: Actual number of pixels (Ground Truth) | Number of Pixel Count: Predicted number of pixels by K-Means with PSO | Number of Pixel Count: TBANN | Accuracy (%): Predicted number of pixels by K-Means with PSO | Accuracy (%): TBANN |
|---|---|---|---|---|---|
| Brocoli_green_weeds_1 | 391 | 271 | 331 | 69.31 | 84.65 |
| Corn_senesced_green_weed | 1343 | 1735 | 1539 | 81.57 | 88.70 |
| Lettuce_romaine_4wk | 616 | 922 | 769 | 75.08 | 83.40 |
| Lettuce_romaine_5wk | 1525 | 2396 | 1960 | 73.34 | 81.84 |
| Lettuce_romaine_6wk | 674 | 1306 | 990 | 67.39 | 75.80 |
| Lettuce_romaine_7wk | 799 | 507 | 653 | 63.45 | 81.73 |

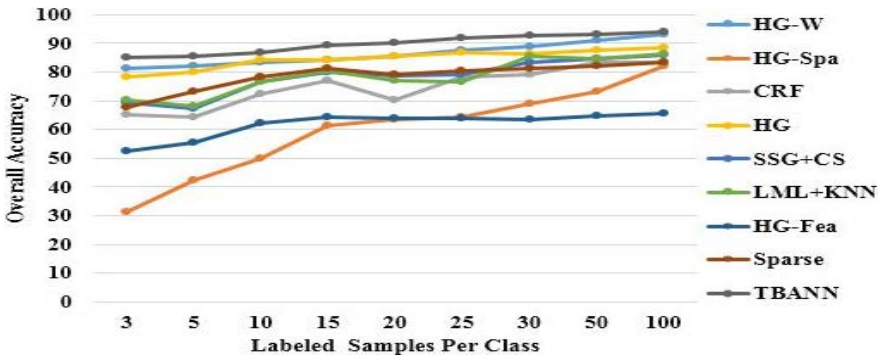


Fig. 7: Overall accuracy analysis

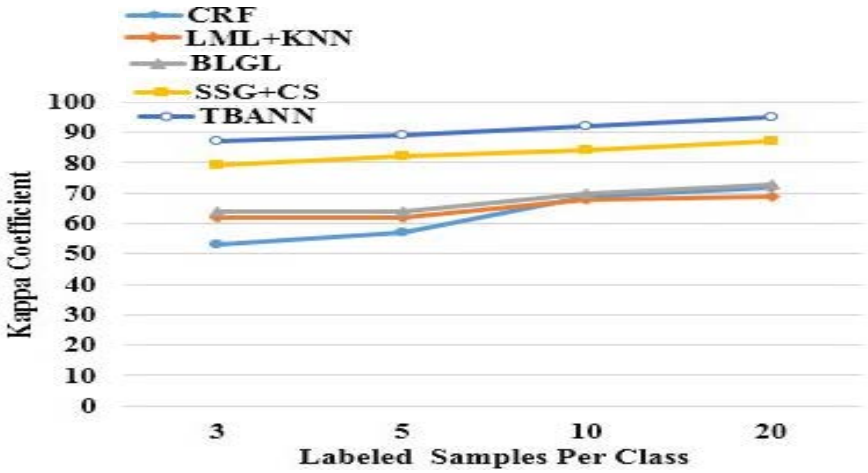


Fig. 8: Kappa coefficient

existing methods CRF, LML+KNN, BLGL and SSG+CS[20]. In existing methods, the SSG+CS provides more Kappa coefficient (87 %) for the maximum number of samples (10). The effective filtering and the NN-based classification in proposed work utilized the PSO-based color feature optimization that provided more Kappa coefficient (95 %) than the existing SSG+CS.

## CONCLUSION

This study discussed the limitations of geological information prediction and Earth monitoring by the satellite images area to preserve the vegetation, weather forecast and the disaster management. The employment of Hyper Spectral Image (HSI) in the various spectral bands offered the significant contribution to the remote sensing applications. The capture of response in HSI in narrow bandwidth caused the less performance. Hence, the number of bands over the various time periods are the important requirement in clear image analysis. The extension of HSI to the multi-temporal images covered more information than RGB image since more bands are available in it. The absence of frames update leads to accuracy degradation. This study focused on multi-temporal images for better isolation of normal and noise region and provided the clear image analysis

compared to HSI. This study proposed the cellular automata-based noise filtering technique with the changes in noise prediction structure to eradicate the noise components, thereby better isolation is achieved. This study overcomes the update and accuracy limitations by an employment of image fusion to each band to eliminate the cloud and provide the necessary updated frames. The classification of normalized images from the fused images by using Tree-Bagger Algorithm with Neural Network (NN) formation (TBANN) predicts the cluster label for the color features of specific band results in the reduction of the atmospheric and signal dependent noise. The comparative analysis between the proposed TBANN with the existing methods regarding the accuracy, Kappa coefficient and the number of pixels count assured the effectiveness of TBANN in remote sensing applications.

## REFERENCES


Bai, J., S. Xiang and C. Pan, 2013. A graph-based classification method for hyperspectral images. IEEE. Trans. Geosci. Remote Sens., 51: 803-817.

Barbin, D., G. Elmasry, D.W. Sun and P. Allen, 2012. Near-infrared hyperspectral imaging for grading and classification of pork. Meat Sci., 90: 259-268.

Bazi, Y., N. Alajlan, F. Melgani, H. AlHichri and S. Malek *et al*., 2014. Differential evolution extreme learning machine for the classification of hyperspectral images. IEEE. Geosci. Remote Sens. Lett., 11: 1066-1070.

Ganesh, B.P., S. Aravindan, S. Raja and A. Thirunavukkarasu, 2013. Hyperspectral satellite data (Hyperion) preprocessing-a case study on banded magnetite quartzite in Godumalai Hill, Salem, Tamil Nadu and India. Arab. J. Geosci., 6: 3249-3256.

Gao, Y., R. Ji, P. Cui, Q. Dai and G. Hua, 2014. Hyperspectral image classification through bilayer graph-based learning. IEEE. Trans. Image Process., 23: 2769-2778.

Ghamisi, P., M.S. Couceiro, F.M. Martins and B.J. Atli, 2014. Multilevel image segmentation based on fractional-order Darwinian particle swarm optimization. IEEE Geosci. Remote Sens., 52: 2382-2394.

Ji, R., Y. Gao, R. Hong, Q. Liu and D. Tao *et al*., 2014. Spectral-spatial constraint hyperspectral image classification. IEEE. Trans. Geosci. Remote Sens., 52: 1811-1824.

Johnson, B.A. and K. Iizuka, 2016. Integrating openstreetmap crowdsourced data and landsat time-series imagery for rapid land use/land cover (lulc) mapping: Case study of the laguna de bay area of the philippines. Appl. Geography, 67: 140-149.

Li, J., P.R. Marpu, A. Plaza, J.M.B. Dias and J.A. Benediktsson, 2013. Generalized composite kernel framework for hyperspectral image classification. IEEE. Trans. Geosci. Remote Sens., 51: 4816-4829.

Merentitis, A., C. Debes and R. Heremans, 2014. Ensemble learning in hyperspectral image classification: toward selecting a favorable bias-variance tradeoff. IEEE. J. Sel. Top. Appl. Earth Obs. Remote Sens., 7: 1089-1102.

Moreno, R., F. Corona, A. Lendasse, M. Grana and L.S. Galvao, 2014. Extreme learning machines for soybean classification in remote sensing hyperspectral images. Neurocomput., 128: 207-216.

Nia, M.S., D.Z. Wang, S.A. Bohlman, P. Gader, S.J. Graves and M. Petrovic, 2015. Impact of atmospheric correction and image filtering on hyperspectral classification of tree species using support vector machine. J. Appl. Remote Sens., 9: 095990-095990.

Tochon, G., J.B. Feret, S. Valero, R.E. Martin and D.E. Knapp *et al*., 2015. On the use of binary partition trees for the tree crown segmentation of tropical rainforest hyperspectral images. Remote Sens. Environ., 159: 318-331.

Valls, G.C., D. Tuia, L. Bruzzone and J.A. Benediktsson, 2014. Advances in hyperspectral image classification: Earth monitoring with statistical learning methods. IEEE. Signal Process. Mag., 31: 45-54.

Villa, A., J. Chanussot, J.A. Benediktsson, C. Jutten and R. Dambreville, 2013. Unsupervised methods for the classification of hyperspectral images with low spatial resolution. Pattern Recognit., 46: 1556-1568.

Wang, Z., N.M. Nasrabadi and T.S. Huang, 2014. Spatial-spectral classification of hyperspectral images using discriminative dictionary designed by learning vector quantization. IEEE. Trans. Geosci. Remote Sens., 52: 4808-4822.

Zhu, Z. and C.E. Woodcock, 2014. Automated cloud, cloud shadow, and snow detection in multitemporal Landsat data: An algorithm designed specifically for monitoring land cover change. Remote Sens. Environ., 152: 217-234.